Flow and thermal characteristics of warm plane air jets (measurements and predictions using different k-ε models)

T. Törnström[1,2,3], S. Amiri[2,4], B. Moshfegh[2,3]
[1]*Department of Energy Technology, SP Swedish National Testing and Research Institute, Borås, Sweden*
[2]*Division of Energy and Mechanical Engineering, Department of Technology, University of Gävle, Gävle, Sweden*
[3]*Division of Energy Systems, Department of Mechanical Engineering, Linköping Institute of Technology, Linköping, Sweden*
[4]*Tekniska Verken i Linköping, Linköping, Sweden*

Abstract

Jets are often used for supplying air to buildings. For designing ventilation systems it is therefore of great importance to have a good understanding of air jets to avoid draught, which might lead to discomfort. At the same time as we want a good indoor climate, we also want to reduce energy consumption.

The purpose of this study is to investigate the flow and thermal characteristics of warm air jets supplied under the ceiling, as a heating method, by means of numerical prediction and full-scale experiments. Together with the warm wall jet, an isothermal wall jet will also be examined. For the calculations, three different k-ε models have been used and evaluated, namely the standard k-ε, the Chen-Kim k-ε model and the Renormalization Group k-ε model. The experiments have been carried out in a full-scale room where the temperature and velocity within the air jet are conducted.

For the isothermal wall jet, the Chen model gives best agreement for the growth rate, while the standard k-ε model gives the best result for the velocity decay of the jet. The evaluation of the warm jet provided best results for the Chen model regarding both the growth rate and the velocity decay. The velocity and temperature profiles for the warm jet provided similar results for all models, but also some differences between the predicted and measured temperatures.

1 Introduction

Large indoor spaces integrated with large glazed surfaces such as shopping centers have become more common. These buildings create a number of heating and cooling problems, both technically and economically. In addition, the current trend of reducing energy consumption has limited the air-conditioned space to merely the areas where activities are concentrated. It is essential when designing ventilation, to have a good understanding of jet behavior to avoid draught in the occupied zone. If one uses a wall jet, discharging along the ceiling, the high velocities can be restricted to the ceiling, thus eliminating discomfort due to ventilation.

The aim of this study is to evaluate the behavior of a warm plane air jet supplied to a room under the ceiling by means of numerical calculations and experiments.

Amiri et al. have made experimental studies on the turbulent warm plane air jet where the effect of cooling loads together with a spectral analysis has been evaluated, see Amiri et al. [1] and Amiri et al. [2]. The result obtained for the isothermal case in an insulated room has been summarized earlier by Karimipanah [3]. This investigation involves both experimental and numerical evaluations. The numerical study was performed for a two-dimensional model.

In this proposed study, the velocity profile and temperature gradient created within the warm air jet will be presented both numerically and experimentally. Also the pressure will be presented in order to evaluate the possibility of predicting the separation point. For comparison, an isothermal wall jet will be calculated.

The employed models are the standard k-ε model by Launder and Spalding [4], the k-ε model by Chen and Kim [5] and the Renormalization Group k-ε model by Yakhot and Orszag [6]. The performance of the turbulence models will be discussed and evaluated. A steady-state three-dimensional model is used for simulating the air movement and the heat transfer in the room. The governing equations are solved by the commercial finite volume code PHOENICS 3.2.

In the near future the behavior of warm and cold wall air jets will be investigated by other turbulence models such as Low-Reynolds-number k-ε model and Reynolds Stress model as well as by Large Eddy Simulations.

2 Numerical procedure

2.1 Physical model

The model under consideration is a well insulated room sized (L×H×W) 6×3×2.95 m, see Figure 1. The inlet is located on the left wall directly under the ceiling and is 0.01 m high and 3.0 m wide. The outlet is also located on

the left wall, close to the floor, 0.04 high and 3 m wide. The heat sink in the room is simulated by a cooling panel placed on the floor, sized 3.6 m long and 1.2 m wide, located along the back wall. The cooling effect to the room is obtained by providing the cooling panel with a surface temperature, *T1*. The temperature of the walls, *T2-T5*, and the temperature of the floor and ceiling, *T6* and *T7* respectively, are the mean values of the surface temperatures measured at five points per surface. The flow is considered steady, turbulent and three-dimensional. Further, the influence of radiation heat transfer is excluded in the present study, due to the constant surface temperature for surrounding surfaces and the participating fluid does not interact with the radiative process.

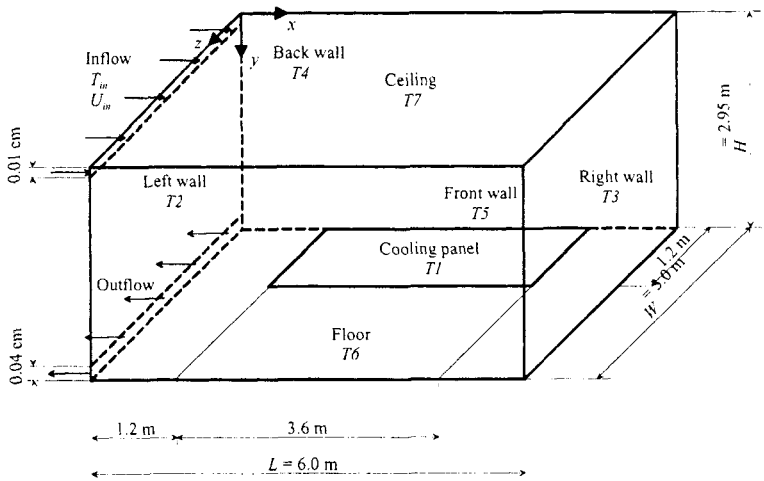

Figure 1. Geometry of the model.

2.2 Governing equations

The instantaneous turbulent flow field in the room is governed by the conservation laws of mass, momentum and energy. After Reynolds averaging and introducing the eddy (turbulent) viscosity the equations get the following form:

$$\frac{\partial}{\partial x_i}(\rho U_i) = 0 \tag{1}$$

$$\frac{\partial \rho U_i}{\partial t} + \frac{\partial \rho U_i U_j}{\partial x_j} = -\frac{\partial P}{\partial x_i} + \frac{\partial}{\partial x_j}\left[(\mu + \mu_t)\frac{\partial U_i}{\partial x_j}\right] + \rho g_i \beta (T_{ref} - T) \tag{2}$$

$$\frac{\partial \rho T}{\partial t} + \frac{\partial \rho U_j T}{\partial x_j} = \frac{\partial}{\partial x_j}\left[\left(\frac{\mu}{Pr} + \frac{\mu_t}{Pr_t}\right)\frac{\partial T}{\partial x_j}\right] + S_t \tag{3}$$

where the turbulent Prandtl number, Pr_t, is 1.0.

2.3 The standard k-ε model

To find an expression for the eddy viscosity, a turbulence model has to be introduced. One of the most widely used models is the standard k-ε model by Launder and Spalding. This model applies two transport equations i.e. the kinetic energy of turbulence k and its dissipation rate ε. This model is hereafter denoted the KE model. The eddy viscosity is defined as, $\mu_t = \rho C_\mu \frac{k^2}{\varepsilon}$. The transport equations for the kinetic energy of turbulence k and its dissipation rate ε, are described as follows:

$$\frac{\partial \rho k}{\partial t} + \frac{\partial \rho U_j k}{\partial x_j} = \frac{\partial}{\partial x_i}\left[\left(\mu + \frac{\mu_t}{\sigma_k}\right)\frac{\partial k}{\partial x_i}\right] + \rho\left(P_k + G_k - \varepsilon\right) \tag{4}$$

$$\frac{\partial \rho \varepsilon}{\partial t} + \frac{\partial \rho U_j \varepsilon}{\partial x_j} = \frac{\partial}{\partial x_i}\left[\rho\left(\mu + \frac{\mu_t}{\sigma_\varepsilon}\right)\frac{\partial \varepsilon}{\partial x_i}\right] + \rho\frac{\varepsilon}{k}\left(C_{1\varepsilon}P_k + C_{3\varepsilon}G_k - C_{2\varepsilon}\varepsilon\right) \tag{5}$$

where the shear production term, P_k, and the buoyancy production term, G_k, are defined as:

$$P_k = \nu_t\left[\frac{\partial U_i}{\partial x_j} + \frac{\partial U_j}{\partial x_i}\right]\frac{\partial U_i}{\partial x_j};\quad G_k = \beta g_i \frac{\nu_T}{Pr_t}\frac{\partial T}{\partial x_i}$$

The model coefficients are (σ_k, σ_ε, $C_{1\varepsilon}$, $C_{2\varepsilon}$, $C_{3\varepsilon}$, C_μ) = (1.0, 1.314, 1.44, 1.92, 1.0, 0.09)

2.4 The Chen-Kim k-ε model

Chen and Kim introduced a modification of the standard k-ε model in order to improve the dynamic response of the ε equation by introducing an additional time scale k/P_k. This allows the ratio P_k/ε to exercise an influence on the production rate of ε and it represents the energy transfer rate from large-scale to small-scale turbulence. The modification also includes the adjustment of several of the standard-model coefficients. This model is hereafter denoted the Chen model. The transport equation for k is identical to the standard model while the equation for ε is as follows:

$$\frac{\partial \rho \varepsilon}{\partial t} + \frac{\partial \rho U_j \varepsilon}{\partial x_j} = \frac{\partial}{\partial x_i}\left[\left(\mu + \frac{\mu_t}{\sigma_\varepsilon}\right)\frac{\partial \varepsilon}{\partial x_i}\right] + \rho\frac{\varepsilon}{k}\left[P_k\left(C_{1\varepsilon} + C_{4\varepsilon}\frac{P_k}{\varepsilon}\right) + C_{3\varepsilon}G_k - C_{2\varepsilon}\varepsilon\right] \tag{6}$$

The model coefficients are (σ_k, σ_ε, $C_{1\varepsilon}$, $C_{2\varepsilon}$, $C_{3\varepsilon}$, $C_{4\varepsilon}$, C_μ) = (0.75, 1.15, 1.15, 1.9, 1.0, 0.25, 0.09)

2.5 The Renormalization Group k-ε model

Yakhot and Orszag derived a k-ε model based on the Renormalization Group (RNG) methods. RNG techniques are used to develop a theory for

the large scales in which the effects of the small scales are represented by modified transport coefficients. A universal random force is employed which drives the small-scale velocity fluctuations and represents the effect of the large scales on the eddies in the inertial range. The modification also includes the adjustment of several of the standard-model coefficients. This model is hereafter denoted the RNG model. The k-equation is identical to the standard model, while the ε equation involves an extra source term R, as follows:

$$R = \frac{C_\mu \eta^3 (1 - \eta/\eta_0)}{1 + \beta\eta^3} \frac{\varepsilon^2}{k}$$

where $\eta_0 = 4.38$, $\beta = 0.012$, $\eta = S\,k/\varepsilon$, $S = (2S_{ij}S_{ij})^{1/2}$ and mean strain rate tensor S_{ij} is defined as:

$$S_{ij} = \frac{1}{2}\left(\frac{\partial U_i}{\partial x_j} + \frac{\partial U_j}{\partial x_i}\right)$$

The model constants are (σ_k, σ_ε, $C_{1\varepsilon}$, $C_{2\varepsilon}$, $C_{3\varepsilon}$, C_μ) = (0.7194, 0.7194, 1.42, 1.68, 1.0, 0.0845).

2.6 Boundary conditions

The boundary conditions are conducted from experimental measurements, see Table 1. The inlet conditions are set with constant velocity, U_{in}, and in the non-isothermal case with a constant temperature, T_{in}. In the non-isothermal case, all surfaces in the room have constant temperature, *T1-T7*. At the walls, the velocity components and the turbulent quantities are set to zero. To predict the turbulent kinetic energy, k_{in}, and its dissipation, ε_{in}, at the inlet the following standard equations are used, see Davidson and Karlsson [7].

$$k_{in} = (0.01 \cdot U_{in})^2, \varepsilon_{in} = 5C_\mu^{0.75} \cdot k_{in}^{1.5} \cdot b^{-1} \tag{7}$$

Table 1. Boundary conditions.

Case	U_{in} (m/s)	k_{in} (m^2/s^2)	ε_{in} (m^2/s^3)	T_{in} (°C)	T1 (°C)	T2 (°C)	T3 (°C)	T4 (°C)	T5 (°C)	T6 (°C)	T7 (°C)
1	13.63	0.019	0.208	-	-	-	-	-	-	-	-
2	10.96	0.012	0.108	23.93	12.00	21.43	21.76	21.50	21.74	21.22	21.89

For the isothermal case the inlet Reynolds number, Re_{in}, is 8689. In the non-isothermal case the inlet Reynolds number is 6988 and the inlet Archimedes number, Ar_{in}, is 4.22×10^{-6}. The inlet Reynolds and Archimedes numbers are defined as:

$$Re_{in} = \rho U_{in} b/\mu\,;\ Ar_{in} = g\beta(T_{in} - T_{ref})b/U_{in}^2$$

where β is the thermal expansion and T_{ref} is the temperature in the middle of the room provided from measurements.

2.7 Numerical solution

The computations were carried out by the commercial CFD code Phoenics 3.2, see Spalding [8]. The governing equations are solved by the finite volume method with a staggered grid system. The hybrid scheme is used for the numerical solution. As a convergence criterion, the sum of the normalized absolute residuals in each control volume for all variables is controlled to be less than 10^{-3}. A non-uniform grid distribution is used with a finer mesh in the near wall region and in the jet-developing region. The number of grid points used at the wall boundaries in the calculation, is chosen so that the values for $y^+ = y \cdot u_\tau / \nu$, for the momentum layer, is kept above 10 over significant parts of the wall boundaries. Grid refinement is applied to check the accuracy of the solution. The grid number was the same for all models and was for the isothermal case 69×33 ($x \times y$) and for the non-isothermal case 69×33×39 ($x \times y \times z$).

3 Experimental procedure

The experiments of this study have been conducted in the specially designed test room at the former Royal Institute of Technology, Gävle, Sweden. The room size is (L×W×H) 6×3×2.95 m, see Figure 1, and it is well insulated from the surroundings.

Air provided by a fan, flows through a heated element and is discharged horizontally through a slot with an aspect ratio (width to height) of 300:1 to form the two-dimensional wall jet. Thus, to simulate an isothermal case, the flow in the mid-plane of the room (z = 1.5 m) can be assumed as a two-dimensional flow. The room is equipped with a cooling panel to absorb the heat delivered to the room by the jet.

The wall surface temperatures, the surface temperature of the cooling panel, local air temperatures, ambient room temperature, and inlet and outlet air temperatures are measured by more than 70 thermocouples. The velocity is measured by a Dantec anemometer 56C01-56C14 and a hot-wire of the type 55R76. Commercially available traversing equipment is used for measuring the local air temperature and velocity at the same time. The local air velocity and temperature are recorded at the different distances from the slot expressed in dimensionless form, x/b = 12, 45, 70, 100, 150, 200, 300 and 400. For more detailed explanation of the experiments, see Amiri et al. (1996) and (1998).

4 Result and discussion

The performances of the three k-ε models are compared with experiments for the isothermal jet, case 1, and for the warm jet, case 2, see Table 1. All the calculated and measured values are obtained in the mid-plane at z = 1.5 m. To reduce the computation-time, the isothermal case has been evaluated using a 2-dimensional model. For validation the Chen model has been used, comparing a 2-dimensional model with a 3-dimensional model yielding very similar result at z = 1.5 m. Therefore a 2-dimensional model is used for the isothermal case for all models.

Velocity and temperature profiles at different downstream distances will be examined and compared. The growth rate and decay rate of the wall jets will be examined. Also the pressure distribution along the ceiling and right wall will be presented for case 2. The purpose is to investigate the possibility to predict the re-circulation zone in the corner between the ceiling and the right wall, see Figure 1, by analyzing the pressure distribution.

4.1 The isothermal case

Figure 2 shows the rate of spread as a function of x/b together with the decay rate as a function of x/b for the isothermal wall jet.

For the growth rate, the distance from the ceiling, y, is normalized by the distance from the ceiling where the velocity has fallen half of its maximum value, $y_{0.5}$. The distance from the inlet, x, is normalized by the inlet slot height b. It is shown from the Figure that all models provide a linear distribution for the growth rate for the isothermal jet, which is in conjunction with the experiments. However all models overpredicts the spread of the jet where the Chen model shows the best agreement with the measured values.

For the decay rate, the maximum velocity of the jet in each location, U_{max}, is normalized by the inlet velocity, U_{in}. Figure 2 shows that all models predict a linear slope in the log scale for the decay of velocity. Compared to the experiments the Chen and KE models provide a similar decay rate, while the RNG model is slightly overpredicting the rate. All the models are overpredicting the velocity throughout the whole domain where the KE model is in best harmony with the measured velocities. The largest difference between numerical and experimental reported values for the velocity is less than 8%, except for the first point x/b = 12, which is rather good. In order to achieve a better agreement between the computations and experimental values, one possible improvement is to use other turbulence models such as Low-Reynolds-number k-ε model with wall damping functions which switch smoothly from laminar to turbulent flow instead of the turbulent wall functions employed in the above-mentioned models.

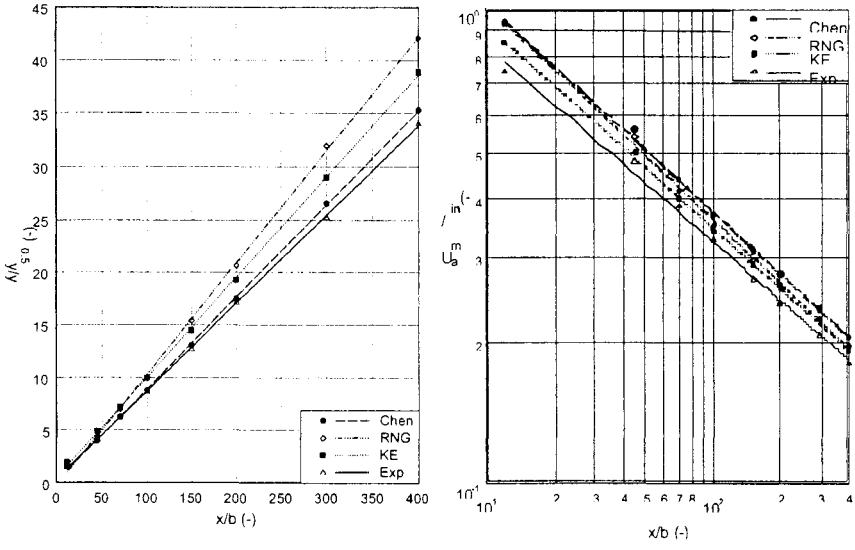

Figure 2. Normalized growth and decay rate for the isothermal wall jet.

4.2 Non-isothermal case

Figure 3 shows the velocity and the temperature profiles at distance x/b = 100 from the inlet.

The velocity, U, have been normalized by the maximum velocity, U_{max}, at the same location. The velocity profiles show similar results for the three models and are in good agreement with measurements. The same results are obtained for the numerical predictions for the other distances from the inlet.

The temperature difference between the local temperature, T, and the room reference temperature, T_{ref}, i.e. $(T\text{-}T_{ref})$ is normalized by the temperature difference between the inlet temperature, T_{in}, and T_{ref}, i.e. $(T_{in}\text{-}T_{ref})$. For the temperature profiles, the employed models show similar results, especially the RNG model and the KE model. The numerical predictions and experiments are in reasonable agreement where the largest differences are located near the ceiling. This might be explained by the difficulty of measuring the air temperature close to walls. The measured temperatures are fluctuating while the calculated values are more homogeneous. The calculated and measured values show similar slopes. The same trends are obtained for other distances from the inlet.

Figure 4 shows the velocity profile for different downstream distances calculated by the Chen model. According to the Figure, the profiles have the same configuration for all downstream locations except for the profile at distance x/b = 12. This can be explained by that the left wall, see Figure 1, affects the jet near the inlet. The same phenomena have been observed by measurements. The other models show the same behavior.

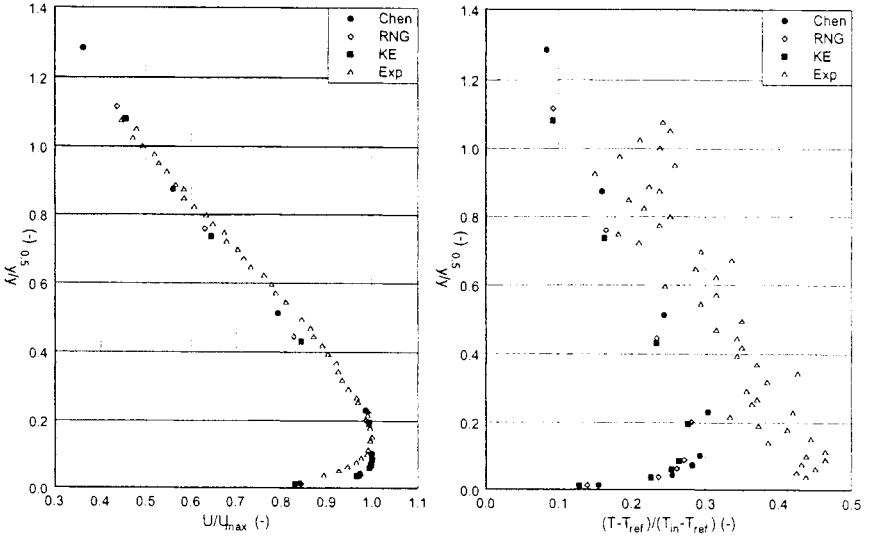

Figure 3. Velocity and temperature profiles for the warm air jet at $x/b = 100$.

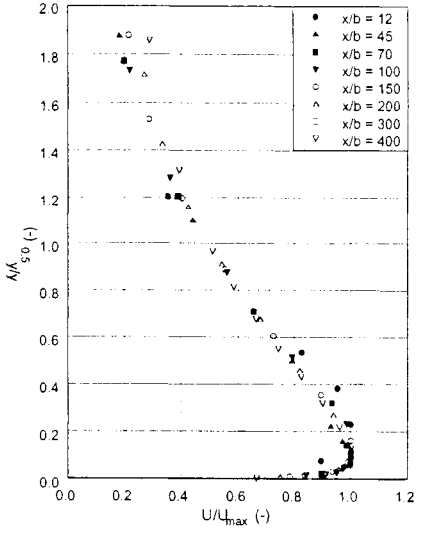

Figure 4. Velocity profiles for the warm air jet predicted by the Chen model.

Figure 5 shows the rate of spread as a function of, x/L_m, together with the decay rate as a function of, x/L_m, for the warm wall jet.

The distance from the inlet, x, is normalized by the thermal length, L_m, that is defined as the distance from an inlet where transition occurs from jet-like to plume-like behavior. The thermal length is defined as, see Etheridge and Sandberg [9]:

$$L_m = b/(Ar_{in})^{2/3} \tag{8}$$

For the growth rate, the same trend as for the isothermal case is observed. All models predict linear spreading rate of the jet and all models are overpredicting the rate. Also for the warm air jet, the Chen model gives results that are in the best agreement with the experiments.

If one look at the decay rate for the warm jet as a function of, x/L_m, it is shown that all models are predicting a linear decay rate in the log scale. The measurements, on the other hand, show a low decay rate in the beginning and a more rapid rate at the end. This difference might be explained by the model's inability to correctly calculate the mixing of a warm jet. All models are underpredicting the velocity except for the first and last location with the Chen and RNG models and the last two locations with the KE model. The Chen model is in best harmony with the measured velocities and the largest difference occurs for x/b = 12 where the difference is 10% and the differences for the other distances is less than 6%, which is rather good.

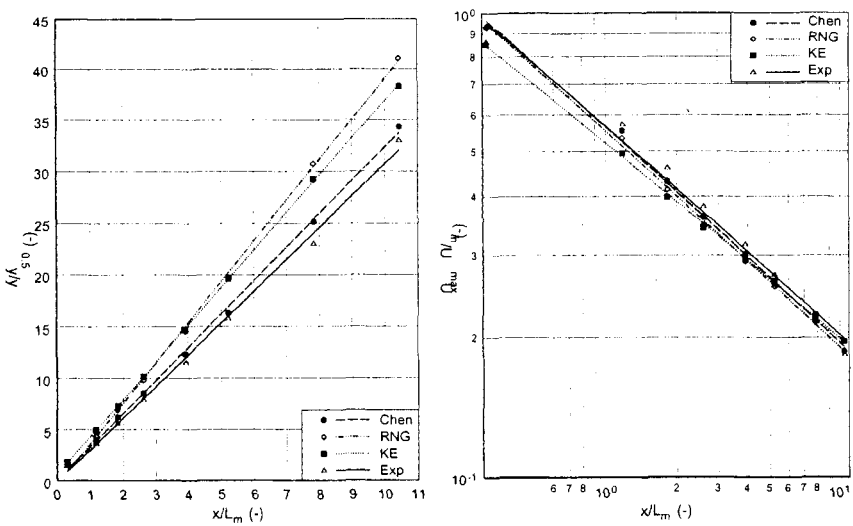

Figure 5. Normalized growth and decay rate for the warm jet.

Figure 6 shows the pressure distribution along the ceiling and the right wall. The pressure is normalized by the product of inlet density and inlet velocity squared.

The models show similar results for the pressure distribution.

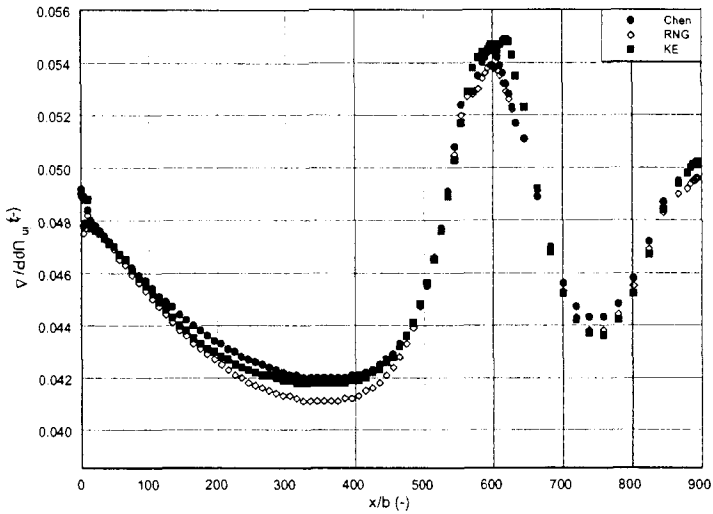

Figure 6. Normalized pressure distribution along the ceiling and the right wall for the warm air jet. Where x/b 0-600 is the ceiling and 600-900 is the right wall starting at the corner.

Since pressure is easy to measure and the CFD calculations provide results of both velocity and pressure, the HVAC engineers can evaluate the separation point by measuring the pressure together with performing numerical predictions. Thus instead of investigating the velocity field only the pressure has to be measured. Unfortunately, no pressure measurements are available at the present time.

5 Conclusions

A great similarity has been observed for the velocity profiles close to the ceiling at different downstream locations from the supply for both cases. The numerical predictions yielded good agreement with the experiments for the normalized velocity for different downstream distances. Prediction of the temperature profiles showed reasonable agreement with experiments for all models. For the isothermal wall jet, the Chen-Kim model provided best agreement with experiments for the growth rate, while the standard k-ε model gave the best result for the velocity decay of the jet. The evaluation of the warm jet provided best agreement for the Chen-Kim model regarding both the growth rate and the velocity decay. For the isothermal case, using

the standard k-ε model, the largest difference between numerical and experimental values for the velocity is less than 8%, except for the first point x/b = 12, which is quite good. For the non-isothermal case, using the Chen-Kim model, the largest difference occurs for, x/b = 12 and the difference is less than 10% and the agreement between predicted and experimental values for other distances is less than 6% which is rather good. Further research on the turbulent warm wall jets is needed e.g. using other turbulence models such as Low-Reynolds number k-ε model and Reynolds Stress model as well as Large Eddy simulations to evaluate the jet behavior.

Acknowledgements

The authors are thankful for the financial support from SP Swedish National Testing and Research Institute (Borås, Sweden), the KK-Foundations (Stockholm, Sweden) and the University of Gävle (Gävle, Sweden).

References

[1] Amiri, S., Sandberg, M. and Moshfegh, B. Effect of Cooling Loads on Warm Plane Air jet. Proceedings of the 5th International Conference on Air Distribution in Rooms, *ROOMVENT'96*, Yokohama, Japan, 1996.

[2] Amiri, S., Sandberg, M. and Moshfegh, B. Spectral Analysis of a Turbulent Warm Plane Air Jet. Proceedings of the 6th International Conference on Air Distribution in Rooms, *ROOMVENT '98*, Stockholm, Sweden, 1998.

[3] Karimipanah, T. Turbulent jets in confined spaces (Application in mixing ventilation, Experimental and Numerical Studies), Ph.D. Thesis, Centre for Built Environment, Royal Institute of Technology, Gävle, Sweden, 1996.

[4] Launder, B.E. and Spalding, D.B. The Numerical Computations of Turbulent Flows. *Comp. Meth. Appl. Mech. Energy* 3, 269-289, 1974.

[5] Chen, Y.S. and Kim, S.W. Computations of turbulent flow using an extended k-ε turbulence closure model, *NASA CR-179204*, 1987.

[6] Yakhot, V. and Orszag, S.A. Renormalization Group Analysis of Turbulence. *J. Sci. Comp.* 1, 3-51, 1986.

[7] Davidson, L. and Karlsson, A. Fluid: *Ett datorprogram för två-dimensionell turbulent strömning*, Publication number 88/6, Department of Applied Thermodynamics and Fluid Mechanics, Chalmers Univeristy of Technology, (in Swedish), 1988.

[8] Spalding, D.B. *The PHOENICS Encyclopedia*, CHAM Ltd, London, U.K., 1994.

[9] Etheridge, D. and Sandberg, M. *Building and Ventilation Theory and Measurements*, John Wiley & Sons, Chichester, U.K., 1996.